NMR Study of Intramolecular Interactions Between Aromatic Groups: Van der Waals, Charge−Transfer, or Quadrupolar Interactions?

ARTICLE *in* JOURNAL OF THE AMERICAN CHEMICAL SOCIETY · SEPTEMBER 1998

Impact Factor: 12.11 · DOI: 10.1021/ja980528s · Source: OAI

Additions and Corrections

NMR Study of Intramolecular Interactions between Aromatic Groups: Van der Waals, Charge-Transfer, or Quadrupolar Interactions? [*J. Am. Chem. Soc.* **1998**, *120*, 9632−9645]. NICHOLAS J. HEATON, PABLO BELLO,† BERNARDO HERRADÓN,* ARÁNZAZU DEL CAMPO, AND JESÚS JIMÉNEZ-BARBERO

Table 2 and Figure 6 were missing in the printed issue and text was duplicated. The full paper follows. Note that the Web publication is complete (Web publication date September 9, 1998).

JA985529Z

10.1021/ja980528s
Published on Web 11/12/1998

NMR Study of Intramolecular Interactions between Aromatic Groups: Van der Waals, Charge-Transfer, or Quadrupolar Interactions?

Nicholas J. Heaton,†,§ Pablo Bello,† Bernardo Herradón,*,‡ Aránzazu del Campo,† and Jesús Jiménez-Barbero‡

Contribution from the Instituto de Ciencia y Tecnología de Polímeros (CSIC) and Instituto de Química Orgánica (CSIC), Juan de la Cierva 3, 28006 Madrid, Spain

Received February 17, 1998

Abstract: Proton nuclear magnetic resonance spectroscopy has been used to investigate intramolecular interactions between different aromatic groups in a series of diesters. The materials investigated comprise two aromatic groups linked by a 2-methyl-1,3-propanedioxy spacer. This spacer permits U-shaped conformations which place the two terminal aromatic groups close together, parallel in a face-to-face arrangement. For the symmetrical diesters, 1,3-bis(9-anthracenecarbonyloxy)-2-methylpropane (**A2**) and 1,3-bis[(3,5-dinitrobenzoyl)-oxy]-2-methylpropane (**N2**), neither the chemical shifts of the aromatic group protons nor the vicinal coupling constants measured in the spacer provide any evidence for a high fraction of U-shaped conformers. In both cases, the conformational distribution of the spacer is similar to that found for 1,3-diacetoxy-2-methylpropane (**M2**), indicating that the planar aromatic groups in **A2** and **N2** experience no significant mutual attractive interactions. In contrast, substantial upfield shifts are observed in the resonance frequencies of all aromatic protons in the anthacenyl and 3,5-dinitrophenyl groups of the unsymmetrical diester, 1-(9-anthracenecarbonyloxy)-3-[(3,5-dinitrobenzoyl)oxy]-2-methylpropane (**AN**), relative to those for the aromatic protons of the respective monoesters and symmetrical diesters. Analysis of the temperature dependence of the vicinal coupling constants indicates highly populated gauche states of the two central C−C bonds of the spacer chain, consistent with a total fraction of U-shaped conformers of about 80% at ambient temperature. Transient nuclear Overhauser effect experiments yield values of between 0.4 and 0.6 nm for average distances between protons on the dinitrophenyl ring and those on the anthracenyl ring, implying a distance of approximately 0.3 nm between the planes of the two aromatic groups. The stabilization of the U-shaped conformers in **AN** is rationalized in terms of quadrupole interactions between the two aromatic groups. The quadrupole moments associated with the two aromatic groups in **AN** have opposite sign, resulting in a significant attractive interaction when the groups are oriented face-to-face. For the symmetrical diesters, **A2** and **N2**, the interacting aromatic groups have identical quadrupole moments and the interaction is repulsive in the face-to-face arrangement.

Introduction

Over the last two decades there has been great interest in the development of polymers which exhibit mesoscopic anisotropy.[1] An important class of such materials is that of semiflexible liquid crystal polymers (LCPs). The first LCPs typically comprised rigid rod-shaped aromatic units connected via flexible methylene, ether, or polysilane chains in linear or comblike structures. More recently, emphasis has been placed on the development of discotic liquid crystal polymers in which the mesogenic group is disc-shaped rather than rod-shaped. In particular, attention has been focused on the role of noncovalent interactions in the

† Instituto de Ciencia y Tecnología de Polímeros.
‡ Instituto de Química Orgánica.
§ Present address: Magnetic Resonance Department, Schlumberger Product Center, 110 Schlumberger Drive, Sugar-Land, TX 77252.

(1) *Polymer Liquid Crystals*; Ciferri, A., Krigbaum, W. R., Meyer, H., Eds.; Elsevier: Amsterdam, 1982. *Side Chain Liquid Crystal Polymers;* McArdle, C. B., Ed.; Blackie: London, 1989.

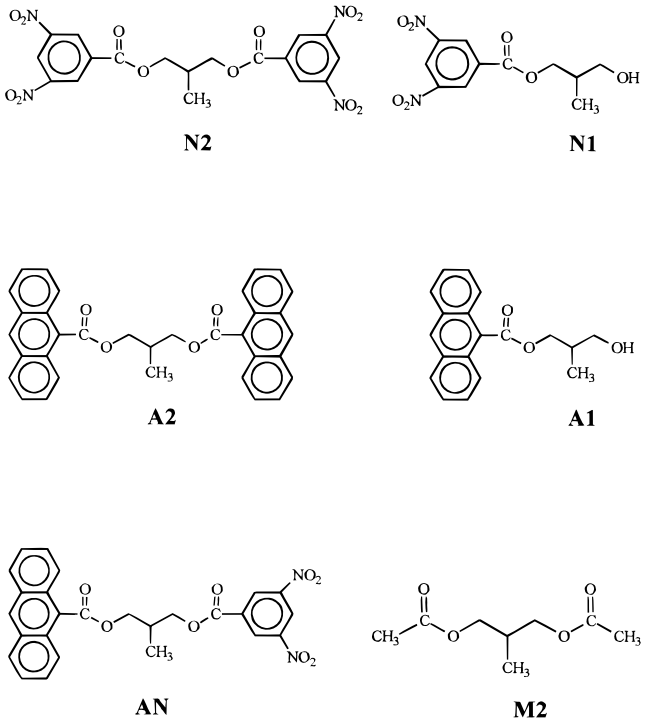

Figure 1. Molecular structures of the diesters and monoesters investigated.

formation of novel supramolecular assemblies.[2] Ringsdorf and co-workers[3] first demonstrated that mesophases could be induced by doping non-liquid-crystalline electron-rich discoid polymers with electron acceptors such as 2,4,7-trinitrofluorenone (TNF). Induced mesophases, also obtained by doping with TNF, have since been observed in low molar mass systems.[4] These results have been rationalized in terms of charge-transfer interactions between the electron donor discoid moieties and the electron acceptor, TNF, which stabilize structures in which the donors and acceptors are stacked alternately. This hypothesis, however, has been questioned by Luckhurst and co-workers,[5,6] who argue that quadrupole interactions between groups with quadrupole moments of opposite sign could also be responsible for the stabilization of the alternately stacked columnar and nematic arrangements. This argument is supported by studies of the binary system of benzene and hexafluorobenzene. An equimolar mixture of the two components yields a crystalline solid with a melting point of 297 K, almost 20 K higher than the melting points of benzene (278.5 K) and hexafluorobenzene (278 K).[7] It was originally thought that the induced crystalline phase exhibited by the mixture was the result of charge-transfer interactions between benzene and hexafluorobenzene molecules. However, no charge-transfer band could be detected in the absorption spectrum of the mixture, an observation which raised serious doubts about this interpretation. In fact, it is now accepted that the columnar structure of the mixture, in which benzene and hexafluorobenzene molecules stack alternately, is due to attractive quadrupolar interactions between the unlike molecules.[8] Computer simulation studies[6] further support the hypothesis that quadrupole interactions between unlike discoid species may play a significant role in determining phase behavior and might also be responsible for the induced mesophases in TNF doped systems.

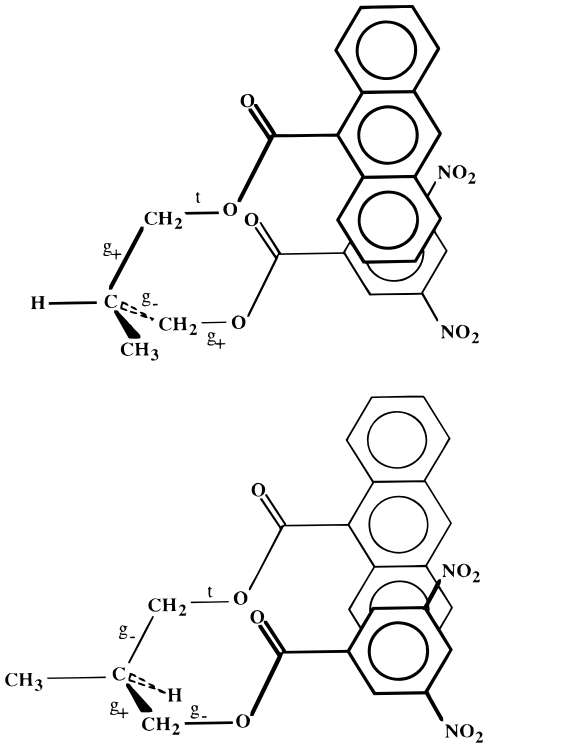

Figure 2. Schematic representations of the structures of U-shaped conformers of **AN**.

The aim of the present work is to provide concrete experimental evidence which could shed useful light on the nature and magnitude of the interactions between different planar aromatic groups. To do this we have prepared a series of diesters of 2-methyl-1,3-propanediol. The molecular structures of the compounds are shown in Figure 1. This flexible spacer was chosen since it has a relatively small total number of conformations and possesses U-shaped configurations which place the terminal ester groups in close proximity. The methyl substituent at the central carbon of the spacer renders the geminal protons of the adjacent methylene groups magnetically inequivalent, which may be exploited for determining vicinal spin coupling constants and thereby estimating chain conformation. In the case of diesters with aromatic terminal groups, the chain geometry for these conformers ensures that the aromatic planes of the two groups are approximately parallel. If we regard the spacer chain within the framework of the rotational isomeric state model, so that each of the four central bonds in the 2-methyl-1,3-propanedioxy spacer may adopt only trans (t), positive gauche (g_+), and negative gauche (g_-) states, then there are just four U-shaped conformers. These have the configurations $tg_\pm g_\pm g_\pm$ and $g_\pm g_\pm g_\pm t$. Two of these configurations for 1-(9-anthracenecarbonyloxy)-3-[(3,5-dinitrobenzoyl)oxy]-2-methylpropane (**AN**) are illustrated schematically in Figure 2. Standard geometry optimization[9] of these U-shaped conformations for **AN** and the analogous configurations in 1,3-bis(9-anthracenecarbonyloxy)-2-methylpropane (**A2**) and 1,3-bis[(3,5-dinitrobenzoyl)oxy]-2-methylpropane (**N2**) gives remarkably

(2) Imrie, C. T. *Trends Polym. Sci.* **1995**, *3*, 22. Tsukruk, V. V.; Wendorff, J. H. *Trends Polym. Sci.* **1995**, *3*, 82.
(3) Ringsdorf, H.; Wüstfeld, R.; Zerta, E.; Ebert, M.; Wendorff, J. H. *Angew. Chem., Int. Ed. Engl.* **1989**, *28*, 914−918.
(4) Praefcke, K.; Singer, D.; Kohne, B.; Ebert, M.; Liebmann, A.; Wendorff, J. H. *Liq. Cryst.* **1991**, *10*, 147−149.
(5) Blatch, A. E.; Fletcher, I. D.; Luckhurst, G. R. *Liq. Cryst.* **1995**, *18*, 801−809.
(6) Bates, M. A.; Luckhurst, G. R. *Liq. Cryst.* **1998**, *24*, 229.
(7) Patrick, C. R.; Prosser, G. S. *Nature* **1960**, *187*, 1021.
(8) Williams, H. W.; Cockroft, K. C.; Fitch, A. N. *Angew. Chem., Int. Ed. Engl.* **1992**, *31*, 1655−1657.
(9) (a) MacroModel 4.5, Columbia University, 1994. (b) Burkett, U.; Allinger, N. *Molecular Mechanics*; American Chemical Society: Washington, DC, 1982.

low values for the respective energies. Calculations employing the MM2 force field[9] yield energies of ~ -5 kJ mol^{-1} (**N2**), ~ -8 kJ mol^{-1} (**A2**), and ~ -6 kJ mol^{-1} (**AN**) for the U-shaped conformers relative to those of the extended all-trans conformers. However, it is emphasized that energy minimization procedures employing standard force fields[9] take account of neither charge-transfer nor quadrupolar terms and make no explicit allowance for solvent molecules. The conformational energies obtained by this kind of approach must therefore be regarded with caution when comparing results with experimental values determined in solution. The remarkably low energies calculated for the U-shaped conformers of **N2**, **A2**, and **AN** derive essentially from the favorable dispersion interactions between atoms in the two terminal groups in close proximity, which add constructively to hold the aromatic planes together at a distance of about 0.3 nm. This effect is not possible for 1,3-diacetoxy-2-methylpropane (**M2**) and is reflected in the much higher relative energies ($\sim +4$ kJ mol^{-1}) for the corresponding U-shaped conformers. Similar results have been obtained previously in molecular modeling studies of polymers and model compounds and have been used to rationalize the degree of excimer formation observed in fluorescence experiments.[10,11]

In this article, we report on the use of liquid-state nuclear magnetic resonance (NMR) to investigate intramolecular interactions between aromatic groups in symmetrical and unsymmetrical diesters. Proton NMR is ideally suited to this task since the proton chemical shifts, coupling constants, and spin relaxation behavior are all influenced by molecular structure and may be exploited independently to probe the underlying intramolecular and intermolecular interactions which determine this structure. Isotropic chemical shift values are governed by the average surrounding electron distribution and are therefore susceptible both to the chemical nature of neighboring substituents in the molecule and to local conformation. They are also dependent to some extent on the solvent. Although it is often difficult to derive precise quantitative information from measurements of chemical shifts, effects can be quite large and hence easily recognized, allowing at least a qualitative interpretation without the need for any spectral simulation or numerical analysis. As in the case of chemical shifts, vicinal spin coupling constants are also governed by the type and relative orientations of neighboring substituents. It has long been recognized that spin coupling constants could provide a reliable probe of conformation in flexible molecules.[12,13] Empirical expressions have been developed which relate the coupling constants to the relative geometry and electronegativity of substituents and to proton−proton dihedral angles.[14,15] These have been successfully employed to investigate conformational distributions in polymers[16] and low molecular weight compounds.[17] Here we are interested in observing U-shaped conformers of diesters of 2-methyl-1,3-propanediol which place the terminal groups in close proximity. The central C−C bonds of the spacer necessarily adopt gauche states in these conformers. It is reasonable to assume that the gauche populations of these bonds, which may be determined by analyzing the respective proton vicinal spin coupling constants, reflect the populations of U-shaped conformers. The nuclear Overhauser effect[18,19] is now routinely employed in a range of chemical and biochemical applications.[20] The effect relies on the cross-relaxation of nuclear spins, and its magnitude is extremely sensitive to internuclear distances of less than about 0.6 nm. In this study we employ transient NOE methods[19] to obtain estimates of the distances between the anthracenyl and 3,5-dinitrophenyl moieties in **AN** and hence obtain a reliable picture of the average structure, which is deternined largely by the interactions between these terminal groups.

Experimental Section

A. Materials. Compounds **M2**, **A2**, **N2**, and **AN** were synthesized from 2-methyl-1,3-propanediol (**DO**) using standard methods. Thus, the diacetate, **M2**, was prepared by acylation with excess acetic anhydride in the presence of pyridine at room temperature and purified by distillation. The diester **A2** was prepared by reaction of **DO** and 2.0 mol equiv of 9-anthracenecarboxylic acid under Mitsunobu conditions (PPh_3, DEAD, THF, room temperature).[21] The main product, **A2**, and byproduct, **A1**, were separated by flash chromatography (hexane/benzene). The reaction of **DO** with 1.5 mol equiv of 3,5-dinitrobenzoyl chloride at low temperature ($Et_3N/CH_2Cl_2/-70$ °C) afforded a ca. 1:1 mixture of **N2** and **N1**, which were readily separated by flash chromatography (hexane/benzene). The monoester, **N1**, was transformed in **AN** by Mitsunobu reaction with 1 mol equiv of 9-anthracenecarboxylic acid. The mixed diester, **AN**, was purified by flash chromatography (benzene/hexane). Although not optimized, all reactions proceeded in high yield (>80%). All the compounds gave satisfactory spectroscopic (copies of the ^{1}H NMR, ^{13}C NMR, and MS spectra are included in the Supporting Information) and analytical data (combustion analysis; C, H, N: ±0.4%).

B. NMR Measurements. Proton NMR spectra were recorded on Varian INOVA 300, INOVA 400, and UNITY 500 spectrometers using benzene-d_6 and DMSO-d_6 as solvents. Coupling constants were determined by fitting experimental spectra with simulated line shapes based on standard expressions for ABX spin systems.[22] A FORTRAN program has been developed for this purpose that employs a nonlinear least-squares fitting routine in which the chemical shifts and respective line widths for spins A, B, and X, as well as the geminal and vicinal coupling constants, are varied simultaneously. Errors in the coupling constants determined in this way are less than 0.05 Hz in all cases. Transient NOE meausurements were carried out for **AN** at 500 MHz using standard procedures.[23] Eight mixing times were employed to follow the buildup and decay of NOEs.

C. Absorption Spectra. Absorption spectra for **N2**, **A2**, and **AN** were recorded in dichloromethane at 300 K on a Perkin-Elmer UV/vis Lambda 16 spectrometer. Spectra were recorded for concentrations ranging from 10^{-7} to 5×10^{-2} mol dm^{-3}.

Results and Discussion

A. Aromatic Proton Chemical Shifts. The aromatic regions of the proton NMR spectra of monoesters **N1** and **A1,** and the corresponding diesters **N2** and **A2,** in benzene-d_6 at

(10) Mendicuti, F.; Kulkarni, R.; Patel, B.; Mattice, W. L. *Macromolecules* **1990**, *23*, 2560−2566.
(11) Martin, O.; Mendicuti, F.; Saiz, E.; Mattice, W. L. *J. Polym. Sci., Part B: Polym. Phys*. **1996**, *34*, 2623−2633.
(12) Gutowsky, H. S.; Belford, G. G.; McMahon, P. E. *J. Chem. Phys*. **1962**, *36*, 3353−3368.
(13) Inomata, K.; Abe, A. *J. Phys. Chem.* **1992**, *96*, 7934−7937.
(14) Karplus, M. *J. Chem. Phys.* **1959**, *30*, 11−15.
(15) Haasnoot, C. A. G.; de Leeuw, F. A. M.; Altona, C. *Tetrahedron* **1980**, *36*, 2783−2792.
(16) Heaton, N. J.; Bello, P.; Bello, A.; Riande, E. *Macromolecules* **1997**, *30*, 7536−7545.
(17) Riande, E.; Jimeno, M. L.; Salvador, R.; de Abajo, J.; Guzmán, J. *J. Phys. Chem.* **1990**, *94*, 7435−7439. Polak, M.; Doboszewski, B.; Herdewijn, P.; Plavec, J. *J. Am. Chem. Soc.* **1997**, *119*, 9782−9792.
(18) Noggle, J. H.; Schirmer, R. E. *The Nuclear Overhauser Effect*; Academic Press: New York, 1971.
(19) Neuhaus, D.; Williamson, M. P., *The Nuclear Overhauser Effect in Structural and Conformational Analysis*; VCH: Weinheim, Germany, 1989.
(20) Würtrich, K. *NMR of Proteins and Nucleic Acids*; Wiley and Sons: New York, 1986. Croasmun, W. R.; Carlson, R. M. K. *Two-Dimensional NMR Spectroscopy. Applications for Chemists and Biochemists*, 2nd ed.; VCH: New York, 1994.
(21) Mitsunobu, O. *Synthesis* **1981,** *1*, 1−28.
(22) Bovey, F. A. *Nuclear Magnetic Resonance Spectroscopy;* Academic Press: San Diego, CA, 1988.
(23) Stott, K.; Stonehouse, J.; Keeler, J.; Hwang, T.-L.; Shaka, A. J. *J. Am. Chem. Soc.* **1995**, *117*, 4199−4200.

298 K, are compared in Figure 3a−d. It is evident that the chemical shifts of the aromatic protons are virtually identical in **N1** and **N2**. Similarly, no significant differences in chemical shift values are observed between the aromatic protons in **A1** and those in **A2**. If the two terminal aromatic groups of the diesters were in close proximity, as would be the case if the U-shaped conformers were highly populated, we should expect to observe marked variations in chemical shifts of the aromatic protons for the monoesters and corresponding diesters. The fact that we do not observe such differences suggests that the two aromatic groups do not interact to any significant degree. This result is in plain contradiction with molecular modeling, which predicts low energies and correspondingly high populations for these conformers.

Figure 3e,f shows the aromatic regions of the proton NMR spectra for an equimolar **N2**/**A2** mixture and **AN**, respectively, in benzene-d_6 at 300 K. The spectrum of the mixture is identical to the sum of the spectra of the individual compounds (Figure 3b,d), indicating the absence of intermolecular complexes between the two components. The spectrum of **AN**, on the other hand, contrasts strikingly with that of the mixture, despite the fact that the aromatic groups are identical in each case. All signals deriving from both the dinitrophenyl moiety and the anthracenyl group in **AN** are shifted upfield by between 0.1 and 0.5 ppm relative to their respective frequencies in the symmetrical diesters and monoesters. The effect is most apparent for the 2′ position doublet in the dinitrophenyl group, which shifts upfield by ∼0.5 ppm and exchanges relative position in the spectrum with the 4′ proton triplet. The variations in chemical shift must derive either from local through-bond effects or from perturbations in the electronic environments as a result of interactions with other molecules or parts of molecules, either solvent or solute. Through-bond effects may be ruled out since the terminal aromatic groups are too far apart. For this reason we find that the aromatic regions of the spectra for the symmetrical diesters and corresponding monoesters are similar. Since all spectra were recorded at high dilution in the same solvent, benzene-d_6, the observed variations in chemical shifts cannot be due to solvent−solute interactions. We therefore conclude that solute−solute interactions are responsible. What is more, the similarity between spectrum 3e, for the **N2**/**A2** mixture, and those for the monoesters and symmetric diesters suggests that these interactions in **AN** are of intramolecular rather than intermolecular origin. Although this result, in itself, does not yield direct information concerning the flexible spacer chain, the U-shaped $tg_{\pm}g_{\pm}g_{\pm}$ and $g_{\pm}g_{\pm}g_{\pm}t$ conformers represent the only physically realistic possibilities which permit significant interaction between the terminal aromatic groups consistent with the anomalous aromatic proton chemical shifts in **AN**.

B. Vicinal Coupling Constants and Chain Conformation. On the basis of the qualitative interpretation of the aromatic proton resonances described above, we conclude that **AN** possesses a high population of U-shaped conformers due to the formation of an intramolecular complex between the anthracenyl and dinitrophenyl terminal groups. As was pointed out above, U-shaped conformers have the configuration $tg_{\pm}g_{\pm}g_{\pm}$ or $g_{\pm}g_{\pm}g_{\pm}t$. We therefore expect the gauche states of the central two C−C bonds of the spacer to be highly populated in **AN**. No similar effect is observed for **N2** or **A2**, and we should not expect abnormal conformational distributions for the respective $-OCH_2$-$CH(CH_3)CH_2O-$ spacers.

The presence of the methyl group attached to the central carbon of the spacer renders the protons in each of the adjacent methylene groups to be magnetically equivalent. Consequently, each $-CH_2CH(CH_3)-$ segment yields an ABX spin system which permits straightforward determination of the vicinal coupling constants, J_{AX} and J_{BX}. Evidently, for the symmetrical diesters, **A2** and **N2**, the two ABX systems corresponding to the $-CH_2CH(CH_3)-$ and $-CH(CH_3)CH_2-$ segments are identical, whereas in the case of **AN** they should yield separate multiplets in the NMR spectrum. Figure 4 shows the methylene resonances corresponding to the AB parts of the ABX multiplets for **N2**, **A2**, and **AN**, recorded at 298 K in benzene-d_6. Each methylene group contributes an octuplet in which the frequencies and relative magnitudes are determined by the chemical shifts, ν_A and ν_B, of the two protons (A and B), the geminal coupling constant, J_{AB}, between them, and the vicinal coupling constants between each of them and the methine (X) proton, J_{AX} and J_{BX}. Although, in general, detailed analysis of second-order spin multiplets requires numerical simulation, we can nevertheless make some broad comparisons of the different multiplets by visual inspection. In each case, the octuplets may be separated into two quartets which are associated with the two protons, arbitrarily designated as A and B. In the remaining discussion we adopt the convention that the A spin is that whose chemical shift appears at higher frequency (i.e., higher ppm) so that $\nu - \nu_B$ is positive. If the two quartets are approximately symmetrically disposed about the central frequency, $(\nu_A + \nu_B)/2$, it follows that the vicinal coupling constants are similar in magnitude. Increasing asymmetry of the two quartets about the center frequency reflects an increasing difference, $|J_{AX-} J_{BX}|$. The methylene multiplets for **N2** and **A2** are indeed approximately symmetric, and we may conclude immediately that the two vicinal coupling constants are not markedly different. In the case of **AN**, we observe two octuplets corresponding to the two chemically distinct methylene groups, as expected. Analysis of the heteronuclear correlation spectrum[24] enables us to assign the well-separated octuplet centered at ∼4.30 ppm as that due to the methylene group adjacent to the anthracenecarbonyloxy group, while the more condensed multiplet at ∼4.05 ppm as that for the methylene protons adjacent to the dinitrobenzoyloxy group. It is remarkable that the chemical shifts of the two protons adjacent to the anthracenecarbonyloxy group are sufficiently different that they yield an almost first-order multiplet at a measuring frequency of 300 MHz. From the clear asymmetry of the octuplet, we can immediately deduce that the vicinal coupling constants differ substantially. Indeed, a simple first-order analysis indicates that J_{BX} is approximately twice as large as J_{AX}. The low frequency multiplet is distinctly second order and precludes any such simple analysis. Numerical best-fit line-shape simulations yield accurate values for the spin coupling constants in all cases.

The relationship between the vicinal spin coupling constants and conformation is illustrated in Figure 5, which shows the projections for each of the rotational isomeric states of the two central C−C bonds of the 2-methyl-1,3-propanedioxy spacer common to all the diesters studied. The protons have been arbitrarily labeled a, b and c, d for the two methylene groups and x for the methine proton to which they couple. Clearly, for the symmetrical diesters, the two bonds are energetically equivalent. They are related by reflection through a mirror plane containing the methyl carbon and methine proton, which implies that the g_+ state of bond 1 is equivalent to the g_- state of bond 2 and has equal energy. Note that no assignment has yet been made regarding the chemical shifts of these protons in any of the compounds. Thus the downfield A spin quartets could

(24) Bax, A., Summers, M. F. *J. Am. Chem. Soc.* **1986**, *108*, 2093−2094.

correspond to proton a or b in the case of methylene group 1. Similarly for methylene group 2, which yields a distinct multiplet in **AN**, the high-frequency A resonances may derive from either proton c or d. Also indicated in Figure 5 are the individual coupling constants, J_i^n and $J_i^{n\prime}$, for the two bonds $n = 1, 2$. Within the framework of the rotational isomeric state model, the vicinal coupling constants, J_{ax} and J_{bx}, are given by

$$J_{ax} + J_{bx} = f^1_{(t)}(J^1_3 + J^{1\prime}_1) + f^1_{(+)}(J^1_1 + J^{1\prime}_3) + f^1_{(-)}(J^1_2 + J^{1\prime}_2) \quad (1a)$$

$$J_{ax} - J_{bx} = f^1_{(t)}(J^1_3 - J^{1\prime}_1) + f^1_{(+)}(J^1_1 - J^{1\prime}_3) + f^1_{(-)}(J^1_2 - J^{1\prime}_2) \quad (1b)$$

where $f^1_{(t)}$, $f^1_{(+)}$, and $f^1_{(-)}$ are the populations of the t, g_+, and g_- states, for bond 1. Similarly, for bond 2 we obtain

$$J_{cx} + J_{dx} = f^2_{(t)}(J^{2\prime}_1 + J^2_3) + f^2_{(-)}(J^{2\prime}_3 + J^2_1) + f^2_{(+)}(J^{2\prime}_2 + J^2_2) \quad (2a)$$

$$J_{cx} - J_{dx} = f^2_{(t)}(J^{2\prime}_1 - J^2_3) + f^2_{(-)}(J^{2\prime}_3 - J^2_1) + f^2_{(+)}(J^{2\prime}_2 - J^2_2) \quad (2b)$$

The populations, $f^n_{(i)}$, are governed primarily by the intramolecular interactions within the chain and are dependent on temperature. In the event that first-order interactions (i.e., interactions between substituents represented in the projections in Figure 5) dominate the intramolecular potential, it is possible to assign unique energies, $E^n_{(\mu)}$, to each of the three conformational states, μ, for bond n and we have

$$f^n_{(\nu)} = [\exp(-E^n_{(\nu)}/RT)]/[\sum_{\mu}\exp(-E^n_{(\mu)}/RT)] \quad (3)$$

If higher order interactions govern the overall intramolecular potential, as may be the case for **AN**, the simple result in eq 3 is no longer strictly valid. However, over the limited range studied, this expression may be employed to approximate the temperature dependence of the populations. The quantities, $E^n_{(\mu)}$, should no longer be regarded as absolute conformational energies but rather statistical averages of the intramolecular energies of the molecules when bond n is in state μ. In principle, these quantities are temperature dependent but their variation between 298 and 338 K is certainly small and can reasonably be neglected for present purposes.

If we regard the trans state as reference configuration, $E^n_{(t)} = 0$, we have a total of eight unknown quantities, the two gauche energies, $E^n_{(+)}$ and $E^n_{(-)}$, and the six coupling constants, J^n_i and $J^{n\prime}_i$ ($i = 1, 2, 3$). At each temperature we can determine just two independent experimental quantities, J_{AX} and J_{BX}. To proceed further with the analysis, it is necessary to make some assumptions concerning J^n_i and $J^{n\prime}_i$. Recalling that these quantities are determined essentially by the relative orientations and electronegativities of substituents and assuming that the bond torsion angles do not deviate significantly from their ideal values of 0, ±120, we now make the approximation $J^{n\prime}_i = J^n_i$. With this simplification and bearing in mind that $f^n_{(t)} + f^n_{(+)} + f^n_{(-)} = 1$, eqs 1 and 2 can be written

$$J_{ax} + J_{bx} = J^1_3 + J^1_1 - f^1_{(-)}(J^1_3 + J^1_1 - 2J^1_2) \quad (4a)$$

$$J_{ax} - J_{bx} = (J^1_3 - J^1_1)(f^1_{(t)} - f^1_{(+)}) \quad (4b)$$

$$J_{cx} + J_{dx} = J^2_3 + J^2_1 - f^2_{(+)}(J^2_3 + J^2_1 - 2J^2_2) \quad (4c)$$

$$J_{cx} - J_{dx} = (J_1{}^2 - J_3{}^2)(f^2_{(t)} - f^2_{(-)}) \quad (4d)$$

These quantities may be compared with the experimental quantities, $J_{AX} + J_{BX} = J_{ax} + J_{bx}$ and $|J_{AX} - J_{BX}| = |J_{ax} - J_{bx}|$ for bond 1. Analogous relations apply for bond 2. Approximate estimates for the J^n_i may be obtained using the empirical expression developed by Altona based on the Karplus equation.[14,15] Assuming ideal torsion angles for each of the conformational states, we obtain $J^1_1 = J^2_1 = 4.1$ Hz, $J^1_2 = J^2_2 = 2.0$ Hz, and $J^1_3 = J^2_3 = 11.5$ Hz. Ambiguity in the assignment of the resonances to the individual protons, a and b (bond 1), is therefore reflected by the uncertainty in the sign of the population difference, $f^1_{(t)} - f^1_{(+)}$. Similarly, for bond 2, the assignment ambiguity leads to an uncertainty in the sign of $f^1_{(t)} - f^1_{(-)}$. In some cases, these uncertainties may be resolved by invoking other evidence concerning conformation and bond energies for this type of chain segment.

Spectra have been recorded in benzene-d_6 and DMSO-d_6 for **N2**, **A2**, **AN**, and the reference compound, **M2**, as a function of temperature between 298 and 338 K. The vicinal coupling constants, determined by fitting the line shapes, are presented in Table 1. Figure 6 shows the temperature dependence of the sum, $J_{AX} + J_{BX}$, and difference, $|J_{AX} - J_{BX}|$, for each compound. As anticipated from the approximate visual analysis of the spectra discussed above, the vicinal coupling constants for **N2** and **A2** are similar with $J_{AX} + J_{BX} \sim 12$ Hz and $|J_{AX} - J_{BX}|$ varying between 0.5 and 0.9 Hz. Similar results are also obtained for **M2**, suggesting that the conformational distributions for all three compounds are similar, determined presumably by essentially the same interactions within the chain. In stark contrast, the $|J_{AX} - J_{BX}|$ values for both methylene groups in **AN** are almost an order of magnitude greater, ranging from 3.5 to 4.7 Hz over the temperature range studied. The fact that the $|J_{AX} - J_{BX}|$ values are large for **AN** is an indication that the two protons in each of the methylene groups sample very different *average* environments. This implies strongly biased population distributions between the trans, gauche(+), and gauche(−) states of both the central C−C bonds.

Estimates have been derived for the $E^n_{(i)}$ by fitting the experimental coupling constants with the expressions in eqs 3 and 4. Because of the large number of unknown parameters involved in the fitting process and the rather limited range of experimental data, it is important to investigate the range of parameter sets which are consistent with experiment. This was achieved by repeating the least-squares fit maintaining J^n_1 and J^n_2 fixed while allowing only $E^n_{(+)}$, $E^n_{(-)}$, and J^n_3 to vary freely. In practice, J^n_1 was fixed at values between 2.0 and 5.0 Hz, while J^n_2 was fixed between 0.5 and 3.5 Hz, which correspond to physically reasonable values for these quantities. Each fit yields a set of energies, a value for J^n_3 and an error. The energies are considered acceptable if the error in the fit is less than or equal to the estimated experimental error and the associated J^n_3 value falls between 10.0 and 13.0 Hz, which are physically reasonable limits for this quantity. The results for **M2**, **N2**, **A2**, and **AN** in the two solvents are presented in Table 2. Note that for the symmetrical diesters (**M2**, **N2**, and **A2**), the energies given refer to bond 1. For bond 2, the gauche energies, $E_{(+)}$ and $E_{(-)}$, are interchanged. In the case of **AN**, results for both bond 1 and bond 2 are given. It was explained above that the ambiguity in spectral assignment leads to uncertainty in the population differences, $f^1_{(t)} - f^1_{(+)}$ and $f^2_{(t)} - f^2_{(-)}$. The results in Table 2 correspond to $f^1_{(t)} - f^1_{(+)} < 0$ and $f^2_{(t)} - f^2_{(-)} < 0$. This choice of assignment is easily justified in the case of **AN**, for which we already have evidence for U-shaped conformers and high gauche populations of the central C−C bonds from the aromatic proton

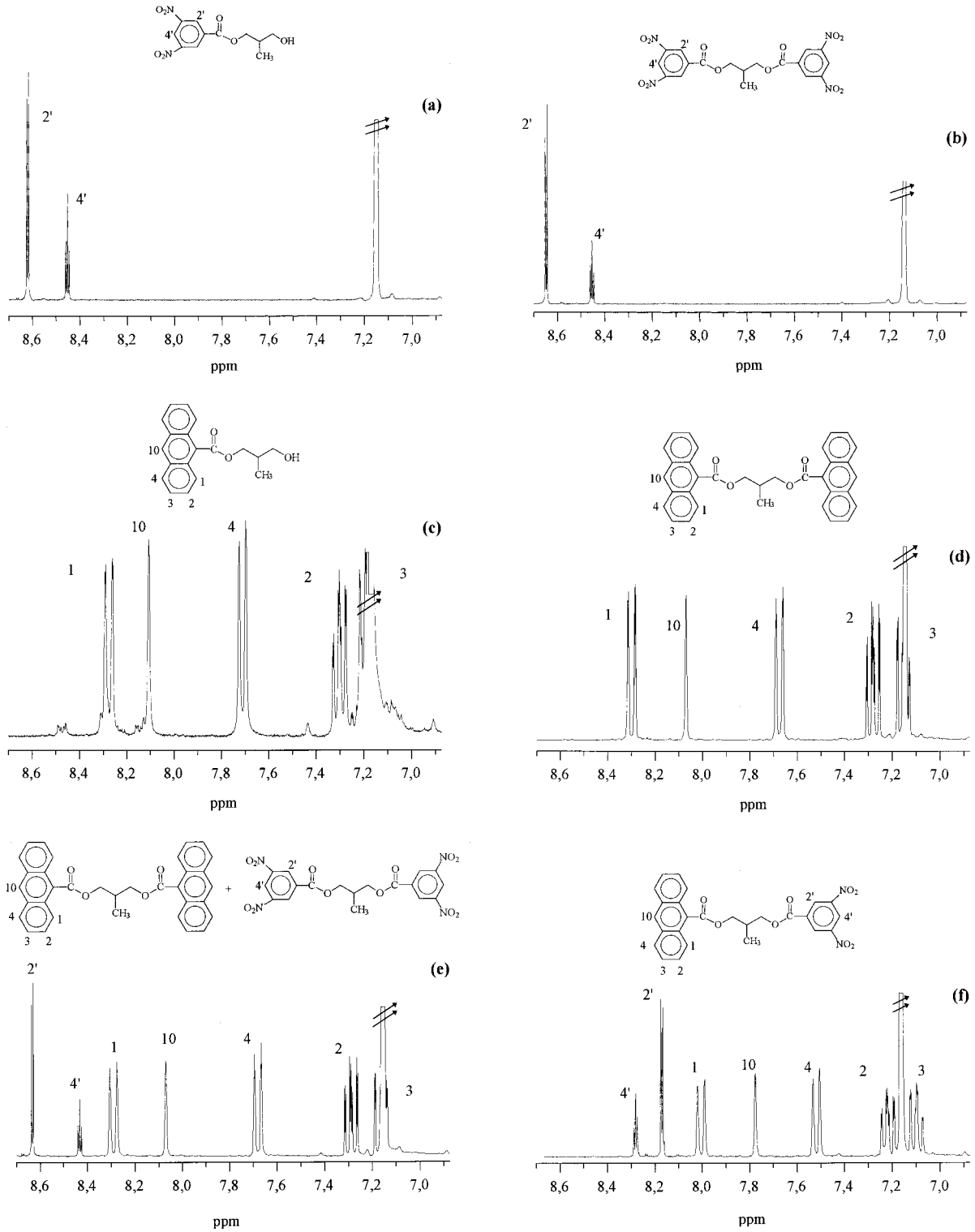

Figure 3. Aromatic regions of the 300-MHz proton NMR spectra of (a) **N1**, (b) **N2**, (c) **A1**, (d) **A2**, (e) 1:1 mixture of **A2** and **N2**, and (f) **AN**. The spectra shown were recorded in benzene-d_6 at 298 K. The solvent peak appears at 7.15 ppm.

chemical shifts (see above). For the symmetrical diesters, the situation is less obvious. Referring to the projection shown in Figure 5, it is reasonable to suppose that the steric interactions associated with g_+ and trans states (bond 1) are very similar. However, charge separation in C−O bonds leaves charges, $\delta+$ and $\delta-$, respectively, on the constituent C and O atoms which would lead to favorable Coulombic interactions betwen non-bonded C and O atoms in gauche orientations. This argument suggests that the g_+ state for bond 1 and g_- state for bond 2 should be of lower energy than the corresponding trans states.

The main conclusion which can be drawn from the results in Table 2 concerns the fundamental difference in conformation between the unsymmetric **AN** and the symmetric diesters (**M2**, **N2**, and **A2**). Although in virtually all cases the gauche states are found to be favored relative to the trans, the magnitudes of the energies are substantially larger in **AN**. The symmetric diesters all display similar values for the respective gauche energies in benzene, suggesting that the primary interactions which govern the conformational distribution are the same in each case. In other words, in the apolar solvent, the terminal

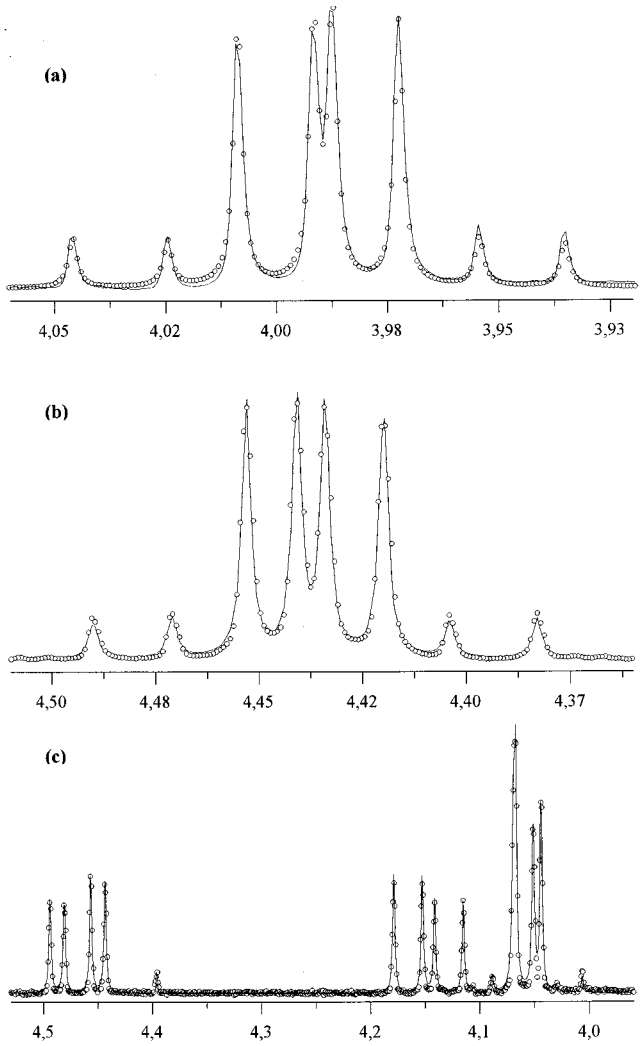

Figure 4. Experimental (open circles) and simulated (solid lines) AB parts of the ABX multiplets due to the methylene groups in (a) **N2**, (b) **A2**, and (c) **AN**. All spectra shown were recorded in benzene-d_6 at 300 MHz and 298 K. The small peak at ~4.4 ppm in part c is due to an unidentified impurity. All other peaks, including the small signals at ~4.05 ppm derive from the methylene groups.

groups do not significantly influence the overall intramolecular potential for these compounds. For **AN**, on the other hand, the potential appears to be dominated by the interaction between the unlike aromatic groups. Assuming that gauche conformations in each of the bonds correspond to U-shaped conformers, we estimate that at least 80% of **AN** molecules adopt these configurations at ambient temperature in benzene. For the reference compound, **M2**, a simple molecular modeling analysis[9a] indicates that less than 1% of molecules adopt U-shaped conformations at ambient temperature.

It is well-known that solvent polarity can play a significant role in determining the conformational distributions of flexible chains. The solvent dependence of vicinal coupling constants derives primarily from the stabilization of certain confomers through dipole−dipole and quadrupole interactions between solvent and solute molecules.[25] Generally, polar conformations are stabilized in solvents with high dielectric constants. Our results indicate that, for both **A2** and **M2**, the trans states of the central C−C bonds are more populated (i.e., gauche energies

(25) Abraham, R. J.; Cavalli, L.; Pachler, K. G. R. *Mol. Phys.* **1966**, *11*, 471−494. Podo, F.; Némethy, G.; Indovina, P. L.; Radics, L.; Viti, V. *Mol. Phys.* **1974,** *27*, 521−539. Viti, V.; Indovina, P. L.; Podo, F.; Radics, L.; Némethy, G. *Mol. Phys.* **1974**, *27*, 541−559.

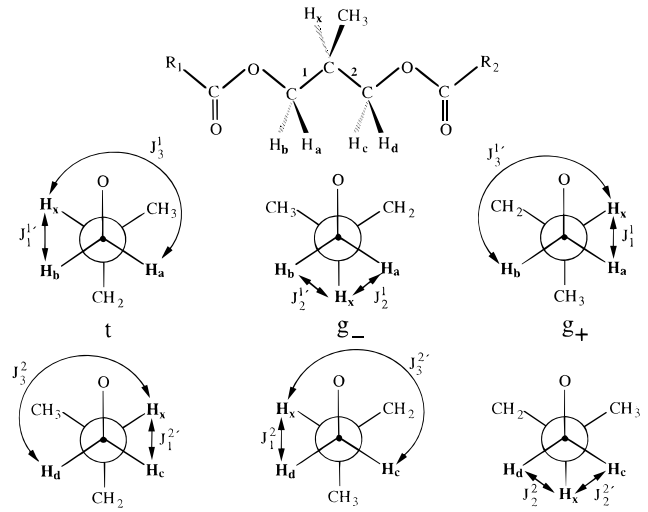

Figure 5. Projections showing the conformation-dependent coupling constants, J_1^n and $J_1^{n\prime}$, between methylene and methine protons in the central C−C bonds of the 2-methyl-1,3-propanedioxy spacer common to all the diesters studied. Projections are shown for bonds 1 and 2, which are mirror images in the symmetric diesters.

Table 1. Vicinal Coupling Constants for the Diesters Measured in Benzene-d_6 and DMSO-d_6 Solutions between 298 and 338 K

	C_6D_6		DMSO-d_6	
T (K)	J_{AX} (Hz)	J_{BX} (Hz)	J_{AX} (Hz)	J_{BX} (Hz)
		M2		
298	6.46	5.75	6.49	5.95
308	6.44	5.76	6.39	5.93
323	6.42	5.78	6.37	5.93
338	6.41	5.82	6.36	5.93
		N2		
298	6.52	5.62	6.52	5.45
308	6.53	5.62	6.63	5.37
323	6.47	5.66	6.61	5.37
338	6.47	5.63	6.59	5.41
		A2		
298	6.46	5.55	6.21	5.92
308	6.44	5.56	6.24	5.93
323	6.35	5.61	6.25	5.93
338	6.61	5.55	6.31	5.91
		AN (Bond 1)		
298	3.60	8.21	4.03	7.66
308	3.70	8.11	4.19	7.53
323	3.83	8.01	4.35	7.36
338	3.95	7.88	4.52	7.24
		AN (Bond 2)		
298	4.09	8.23	4.09	7.56
308	4.14	8.23	4.36	7.46
323	4.26	8.11	4.53	7.33
338	4.37	7.97	4.74	7.25

are less negative) in the polar solvent (DMSO) than in the apolar solvent (benzene), while the opposite effect is observed for **N2**. This result can be rationalized qualitatively by considering the polarity of each of these molecules in the all-trans state. The dipole moment of the ester group is estimated to be 1.89 D and lies approximately along the carbonyl bond.[26] In the planar all-trans conformations of **M2** and **A2**, the dipole moments of the two ester groups are almost parallel so that the overall dipole moment for the molecule is maximized, as illustrated in Figure 7. It is to be expected that these polar all-trans conformations are stabilized in polar solvents. This prediction is in agreement

(26) Saiz, E.; Hummerl, J. P.; Flory, P. J.; Plavsic, M.; *J. Phys. Chem.* **1981**, *85*, 3211−3215.

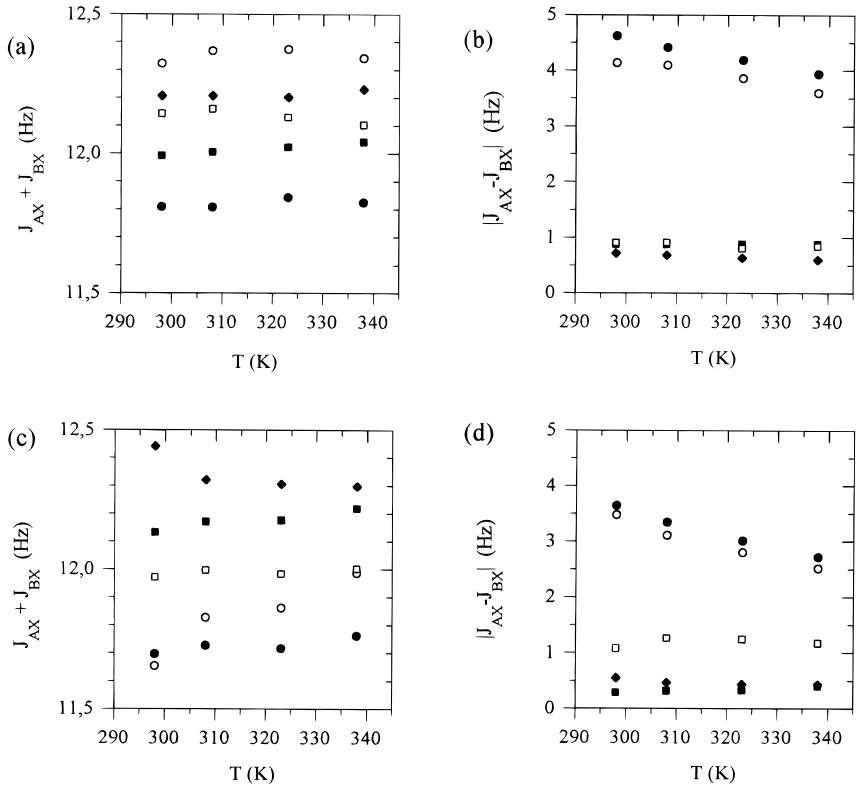

Figure 6. Temperature dependence of the sum and difference values of the vicinal coupling constants measured for **M2** (◆), **N2** (□), **A2** (■), **AN** (bond 1) (●), and **AN** (bond 2) (○) in benzene-d_6 and DMSO-d_6: (a) $J_{AX} + J_{BX}$ measured in benzene-d_6; (b) $|J_{AX} - J_{BX}|$ values in benzene-d_6; (c) $J_{AX} + J_{BX}$ measured in DMSO-d_6; (d) $|J_{AX} - J_{BX}|$ values in DMSO-d_6.

Table 2. Average Conformational Energy Values Determined by Fitting Vicinal Coupling Constant Data Measured in Benzene-d_6 and DMSO-d_6 Solutions

	benzene-d_6		DMSO-d_6	
compd	$E_{(+)}$/J mol^{-1}	$E_{(-)}$/J mol^{-1}	$E_{(+)}$/J mol^{-1}	$E_{(-)}$/J mol^{-1}
M2[a]	-700 ± 200	-450 ± 150	-450 ± 100	$+200 \pm 200$
N2[a]	-900 ± 300	-200 ± 150	-1400 ± 400	-1200 ± 400
A2[a]	-900 ± 300	-600 ± 200	-300 ± 150	-400 ± 250
AN[b]	-5000 ± 2000	-4000 ± 2500	-3500 ± 1500	-3000 ± 1000
AN[c]	-3500 ± 1500	-4500 ± 2000	-2500 ± 1000	-3200 ± 800

[a] Results for symmetric diesters refer to bond 1 (see Figure 5). [b] Bond 1. [c] Bond 2.

with the observed solvent dependence of the conformational energies for **M2** and **A2**. The dipole moment for *m*-dinitrobenzene is about 3.8 D[27] and lies along the symmetry axis of the ring. Adding to this the dipole moment due to the ester group we estimate a total dipole for the dinitrobenzoyloxy group of about 3.3 D, oriented at approximately 30° to the para axis of the aromatic ring. It is evident in Figure 7 that for **N2** in the all-trans conformation the dipoles of the two dinitrobenzoyloxy groups are virtually antiparallel and the overall dipole moment of the molecule is necessarily small. Again, this is consistent with the observed result that the trans states of the central C−C bonds of **N2** are disfavored in the more polar solvent. For **AN**, the situation is less obvious since the all-trans conformer is barely populated in either benzene or DMSO and could not be responsible for the observed solvent dependence. According to our analysis, the most populated conformers are the U-shaped conformers. For these, the dipole moments of the aromatic ester groups are approximately orthogonal. Without performing a more rigorous conformational analysis, it is not possible to

(27) McClellan, A. L. *Tables of Experimental Dipole Moments*; Rahara Enterprises: California, 1973; Vol. 2.

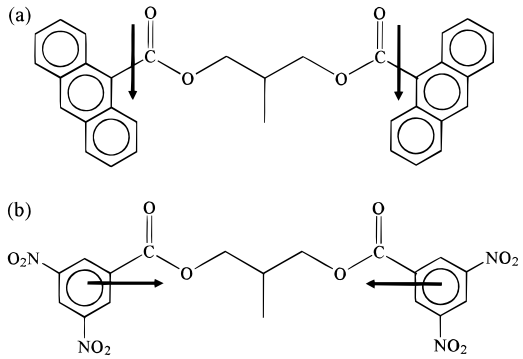

Figure 7. Relative orientations of group dipole moments for (a) **A2** and (b) **N2** in the all-trans configurations. The group dipole moments in **M2** (not shown) are similar to those for **A2**.

derive detailed structural information from the observed solvent dependence of the conformational energies in **AN**. However, we note that the U-shaped conformers seem to exhibit a preference for apolar solvents, suggesting that these configurations possess relatively low total dipole moments.

It is to be expected that the methyl group influences the conformational distribution of the spacer and most probably provides some stabilization of the U-shaped conformers. However, the effect is almost certainly small compared with the stabilization energy resulting from the interaction between the aromatic groups. The very fact that large differences in conformation are observed between the symmetric and unsymmetric diesters, all of which contain the same spacer chain, including the methyl group, supports this hypothesis. Molecular mechanics calculations also indicate that the influence of the methyl group should be of secondary importance, in these compounds. In contrast, for longer spacers or diesters with small

nonaromatic end groups, the methyl group may be expected to have a greater influence on the conformation.

C. Structure of Intramolecular Complex in AN via NOE Measurements. The results concerning aromatic proton chemical shifts and vicinal spin coupling constants provide clear evidence for intramolecular complex formation in **AN**. These complexes are associated with U-shaped spacer conformations which place the terminal aromatic groups parallel and in close proximity. More detailed evidence for the structure of this complex can be obtained by determining the NOEs between protons on the two different aromatic groups. Referring to Figure 3f, we see that all aromatic protons in **AN** yield well-resolved peaks in the NMR spectrum recorded at 298 K in benzene-d_6. Transient NOE experiments can readily be performed by selectively inverting one of the peaks and monitoring the subsequent relaxation and transfer of magnetization by simply recording spectra as a function of time following the inversion.[19] The time dependence of the longitudinal magnetization following the monitoring pulse is given by solving the master equation for spin diffusion:[28]

$$d\mathbf{M}/dt = -\mathbf{RM} \tag{5}$$

In eq 5, the elements, M_i, of vector **M** are the magnetization components for protons i and are proportional to the corresponding peak integrals. The relaxation matrix, **R**, has elements[28]

$$R_{ii} = C\left[\frac{2(n_i - 1)}{\langle r_{ii}^{\,6}\rangle}(J(\omega_0) + 4J(2\omega_0)) + \sum_j \frac{n_j}{\langle r_{ij}^{\,6}\rangle}({}^2/_3 J(0) + 2J(\omega_0) + 4J(2\omega_0))\right] + R_A \tag{6a}$$

$$R_{ij} = C\left[\frac{n_i}{\langle r_{ij}^{\,6}\rangle}(4J(2\omega_0) - {}^2/_3 J(0))\right] \tag{6b}$$

where r_{ij} is the distance between protons i and j, n_i is the number of magnetically equivalent protons of type i, and C is the proton−proton dipolar relaxation strength constant:

$$C = \frac{3\gamma_H \hbar^4}{4}\left(\frac{\mu_0}{4\pi}\right)^2 \tag{7}$$

The additional relaxation rate, R_A, is included to account for other interactions not explicitly included in the analysis. The spectral densities, $J(\omega)$, are defined here as

$$J(\omega) = {}^1/_5\left(\frac{\tau}{1 + \omega^2\tau^2}\right) \tag{8}$$

It has been implicitly assumed that the molecular dynamics may be described by a single rotational correlation time, τ. For low molecular weight molecules, such as **AN**, the error due to this approximation is small, particularly for the U-shaped conformers, which are presumably close to spherical in shape.

Equations 6−8 show that the relaxation matrix elements are determined by the interproton distance parameters, $\langle r_{ij}^{-6}\rangle$, the correlation time, τ, and the additional relaxation rate, R_A. For protons whose nearest neighbors are less than about 0.3 nm away, the additional relaxation term should be small relative to the explicit terms in eq 6. For protons with no close neighbors, however, this term may be important and must be included in the analysis. For simplicity, we assume here that R_A is identical for all protons i. The solution to eq 5 can be written as

$$\mathbf{M}(t) = \mathbf{U}[e^{-\lambda t}]\mathbf{U}^{-1}\mathbf{M}(0) \tag{9}$$

where λ are the eigenvalues of **R** and **U** is the matrix which contains the corresponding eigenvectors. The procedure adopted for the analysis of the transient NOE experiments for **AN** involved fitting the measured peak integrals over a range of mixing times, t, using eq 9. The variable parameters employed in the fit are the interproton distance parameters, $\langle r_{ij}^{-6}\rangle$, the rotational correlation time, τ, and the relaxation rate, R_A. Only aromatic protons were considered explicitly in the fitting process. Relaxation via interactions with aliphatic protons is accounted for in R_A. Distances between protons within the same aromatic groups were obtained from a standard molecular model package[9a] and were not varied during the fit. Two separate experiments were performed. In the first experiment, the peak corresponding to proton 10 in the anthracenyl moiety was inverted (see Figure 3f). For the second experiment, the peak corresponding to proton 4′, the para position in the 3,5-dinitrophenyl group was inverted. In each case, eight mixing times between 0.3 and 5.6 ms were employed.

Figure 8 shows the experimental results and best fit profiles for the two experiments. Parts a and b, respectively, of Figure 8 contain the magnetization decay profile for proton 10 and the cross-relaxation NOE profiles for protons 4 and 3 within the same anthracenyl group, measured during the first experiment. Note that the three best-fit profiles corresponding to self-relaxation (proton 10), nearest neighbor cross-relaxation (proton 4), and the three-spin relayed diffusion (proton 3) are all governed essentially by a single parameter, namely the correlation time, τ. All relevant interproton distances are known quantities which were not varied in the fit while the relaxation rate, R_A, is relatively small compared to self- and nearest neighbor cross-relaxation mechanisms within the anthracenyl group. Figure 8c shows the transient NOE peak profiles for protons 2′ and 4′ on the dinitrophenyl group measured in the same experiment. The fact that significant cross-relaxation occurs between proton 10 and protons 2′ and 4′ shows beyond doubt that the two aromatic groups in **AN** are maintained in close proximity. This is supported further by the results in Figure 8d which show the NOE profiles for protons 4, 10, and 1 obtained in the second experiment (inversion of peak 4′). The NOE profile for proton 1 in this experiment is poorly defined due to low signal/noise. However, a small NOE is clearly observed for $t < 3$ s and warrants inclusion in the analysis. Note that all best-fit profiles shown in Figure 8 were obtained with the same set of parameters. A value of 30 ± 2, estimated from the self-relaxation of proton 4′, was found to be 0.12 s^{-1}. The interproton distances determined in the analysis are presented in Table 3.

On the basis of these results it is possible to estimate the structure of the intramolecular complex. A simple error minimization procedure was developed in which the NOE data was fit by varying the position and orientation of the dinitrophenyl group relative to the anthracenyl group. Structures for the separate aromatic groups were taken from a commercial molecular modeling package.[9a] This procedure implicitly assumes a unique geometry for the complexes formed in the U-shaped conformers. As pointed out previously, there are actually four chain configurations which give rise to U-shaped conformers, namely $tg_{\pm}g_{\pm}g_{\pm}$ and $g_{\pm}g_{\pm}g_{\pm}t$. The $g_+g_-g_+t$ and $g_-g_+g_-t$ conformers would be mirror images, were it not for the presence of the methyl group at the central carbon of the

(28) Macura, S.; Ernst, R. R. *Mol. Phys.* **1980**, *41*, 95−117.

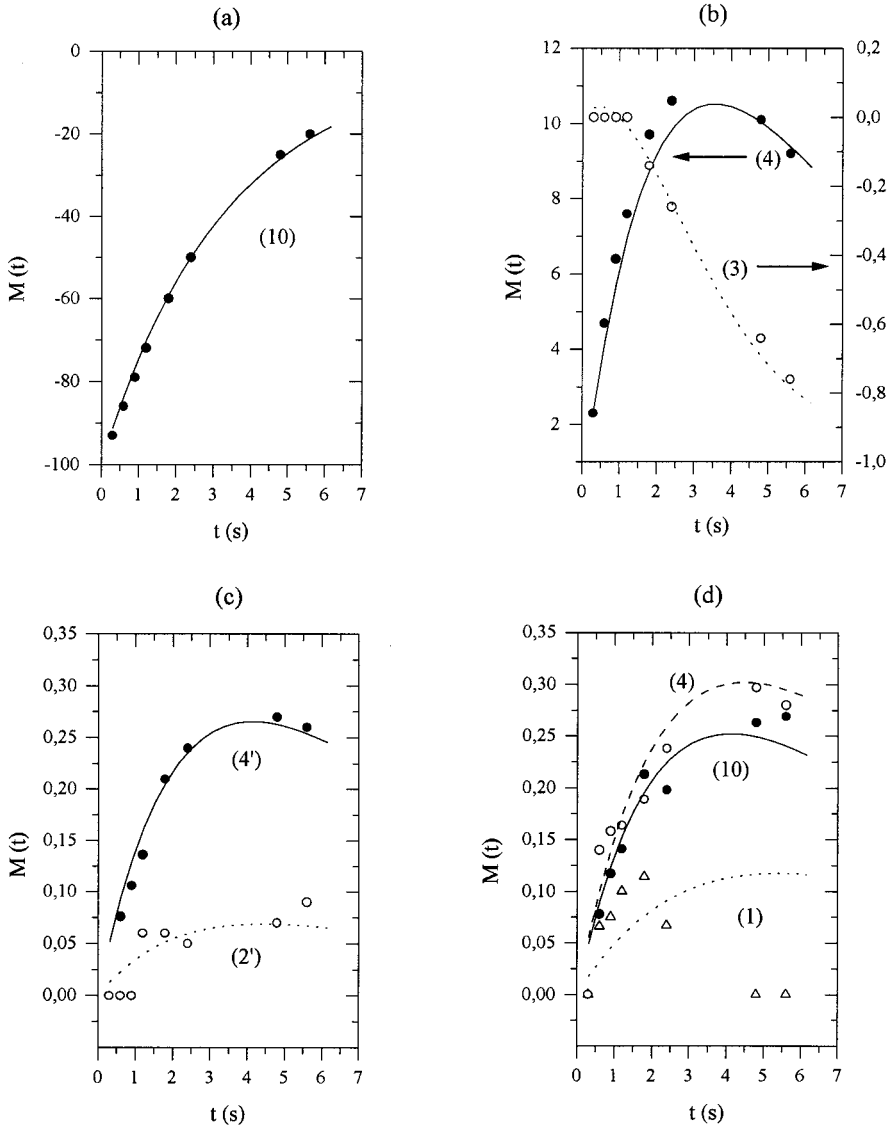

Figure 8. NOE profiles measured for **AN** in benzene-d_6 at 298 K and 500 MHz. (a) Recovery of proton 10 magnetization (anthracenyl group) following inversion. (b) NOE profiles for protons 4 and 3 (anthracenyl group) following inversion of proton 10 peak. (c) NOE profiles for protons 4′ and 2′ (dinitrophenyl group) following inversion of proton 10 peak. (d) NOE profiles for protons 4, 10, and 1 (anthracenyl group) following inversion of peak 4′ (dinitrophenyl group). Solid and broken lines correspond to best-fits obtained using eq 9. All best-fit profiles were obtained with the same set of parameter values (r_{ij}, t, and R_A).

Table 3. Interproton Distances[a] between Protons on Opposite Terminal Aromatic Groups of Unsymmetric Diester, AN, Determined from Transient NOE Measurements

anthracenyl group proton *i*	dinitrophenyl group proton *j*	interproton distance $(\sqrt[6]{\langle r_{ij}^{-6}\rangle})^{-1}$ (nm)
10	2′	0.52
10	4′	0.41
4	4′	0.45
1	4′	0.55

[a] Error limits of less than ±0.02 nm are estimated for all interproton distances except $r_{14'}$, which has an error of about 0.03 nm. The larger error in this case is due to the small NOE observed between protons 1 and 4′.

spacer, which breaks the symmetry of the spacer chain. Similarly, the $tg_+g_-g_+$ and $tg_-g_+g_-$ configurations would also be energetically equivalent. However, the perturbation due to the methyl group may be taken to be small relative to the interactions between the aromatic groups and we can therefore assign a single geometry to the $tg_\pm g_\pm g_\pm$ configurations and another to the $g_\pm g_\pm g_\pm t$ conformations. The relative orientations of the two aromatic groups and the energies of the resulting complexes are presumably different in the two cases. Our assumption of a single structure for the complex is therefore equivalent to assuming that the energy difference between the two possible structures is either very large or negligible. In the case of a negligible energy difference, the geometries of the complexes should also be equivalent. The validity of the assumption is difficult to judge without prior knowledge of the physical nature of the interaction responsible for complex formation. However, with the limited interproton distance data available, the unambiguous determination of two independent geometries and corresponding statistical weights is not feasible in practice.

The structure of the intramolecular complex, obtained by fitting the NOE data, is illustrated schematically in Figure 9. Interestingly, the dinitrophenyl ring is found to be centered almost directly above the central ring of the anthracenyl group. A distance of 0.31 nm is estimated between the central point of the dinitrophenyl ring and the anthracenyl plane, and an angle of about 20° is found between the para axes of the two aromatic groups. These results were obtained assuming an overall

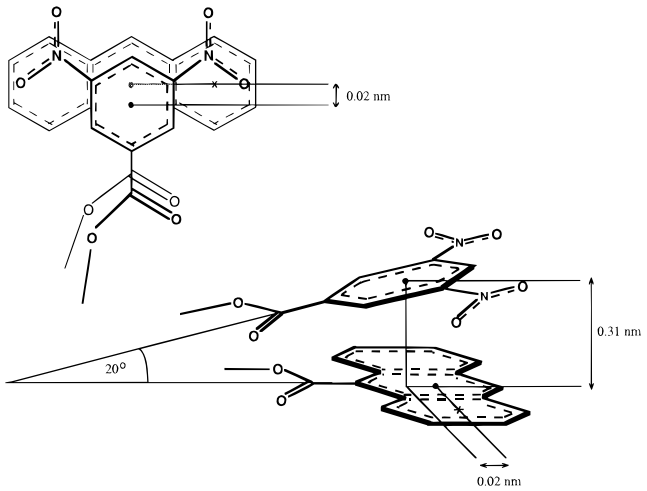

Figure 9. Approximate structure of intramolecular complex in **AN** estimated from interproton distance data derived from the analysis of NOE experiments

statistical probability, ρ, of 80%, for the complex forming configuration, consistent with the conformational energies estimated by fitting the vicinal coupling constants. Increasing ρ from 60% to 90% results in an increase in the estimated distance between the aromatic planes from 0.25 to 0.33 nm while the angle between the aromatic planes decreases from 30° to 18°. The interplanar separation and angle are both sensitive to the measured distance between protons 1 and 4′. Unfortunately, this quantity is rather poorly defined due to the small NOE observed between these protons. We note that an increase in $r_{14'}$ from 0.55 to 0.60 nm, maintaining all other distances identical, leads to an increase in the estimated interplanar separation from 0.30 to 0.34 nm and a decrease in the interplanar angle from 20° to 10°. Taking account of these reasonable margins of error, the structure obtained here for the intramolecular complex in **AN** is comparable with the structures of TNF-doped discotic phases,[29] where an average intermolecular distance of 0.34 nm is estimated.

D. Origin of the Intramolecular Complex in AN. The results presented above establish beyond doubt the existence of a stable intramolecular complex between the dinitrophenyl and anthracenyl rings in **AN**. We now turn our attention to the question of the nature of the interaction responsible for the formation of this complex. Three candidates for the interaction are dispersion (Van der Waals), charge-transfer, and quadrupolar interactions.

The first of these can be ruled out immediatedly, however, since we do not observe any shifts in the aromatic protons in either **N2** or **A2** and the respective spacer chains show no propensity to form U-shaped configurations. If Van der Waals interactions were dominant, we should expect to observe the greatest effect in **A2**, which has the largest planar aromatic groups. Indeed, this is the result provided by molecular mechanics and molecular dynamics simulations conducted in vaccuum, where the long-range nonbonded interactions are accounted for by Coulombic, dipolar, and dispersion contributions. The results obtained in the present NMR study for dilute solutions, however, are in plain contradiction with these predictions and raise serious doubts concerning the validity of standard molecular modeling and dynamics simulations of isolated molecules for rationalizing intramolecular complex formation and conformational behavior in systems containing aromatic groups.[10,11]

Charge-transfer complexes formed by combining electron-deficient nitro-containing aromatic groups with electron-rich aromatic acceptor molecules are well-known. An early example of such a complex is that formed between trinitrobenzene and benzene.[30] Evidence for the existence of the complex in this case is provided by the appearance of a well-defined band in the absorption spectra of the benzene/trinitrobenzene mixture, absent in the spectra of the individual components.[30] More recent examples of charge-transfer complexes involving nitro-substituted aromatics are the induced mesophases obtained by doping electron-rich discoid materials with TNF.[3,4] The possibility of intramolecular charge-transfer complexes involving TNF-containing flexible molecules has also been demonstrated.[29,31,32] All these systems studied comprise strong donor as well as powerful acceptor groups. In the case of **AN**, the dinitrobenzoyl group is undoubtedly a good electron acceptor. The anthracenecarbonyl group, however, does not generally behave as a donor. Indeed, it is known to act as an electron acceptor in some intramolecular energy transfer complexes.[33] Therefore, purely on the basis of these chemical observations, some doubts are raised concerning the likelihood of significant charge-transfer interactions taking place in **AN**.

Charge-transfer complexes are generally detected by the appearance of new bands in the absorption spectrum, often in the visible region, which are not present in the spectra of the individual components.[32,34,35] The absorption spectra of **N2**, **A2**, and **AN** between 200 and 400 nm in dichloromethane (10^{-5} mol dm^{-3}) are presented in Figure 10. None of the compounds presents any absorption peaks in the visible region up to 900 nm. It is significant that the **AN** spectrum does not contain any bands other than those exhibited by **N2** and **A2**. In their study of charge-transfer complexes in discotic liquid crystal/TNF systems, Markovitsi et al. suggested that intramolecular charge-transfer interactions can have low molar absorption coefficients and for this reason may be difficult to identify.[32] However, spectra have been recorded at concentrations of up to 0.05 mol dm^{-3} and we observe no absorption in any of the compounds between 400 and 900 nm. The only significant aspect of the **AN** spectrum is the slight broadening of the anthracene bands which occur at about 350 nm (see Figure 10d). Preliminary experiments also indicate an efficient quenching of the anthracene flourescence.[36a] This is presumably a result of the proximity of the two aromatic groups in the intramolecular complex, although there is no evidence to suggest that this complex is due to a charge-transfer process. On the other hand, we note that, although both **A2** and **N2** give colorless solutions in benzene, **AN** gives a yellow solution. However, many anthracene derivatives display a similar yellow color and this observation for **AN** may not be the result of a charge-transfer complex. In connection with this, we remark that an intramolecular complex, similar to that described here for **AN**, has also been identified in 3-(benzyloxy)-1-[(3,5-dinitrobenzoyl)oxy]-

(29) Möller, M.; Tsukruk, V. V.; Wendorff, J. H.; Bengs, H.; Ringsdorf, H. *Liq. Cryst.* **1992**, *12*, 17−36.

(30) Lawrey, D. M. G.; McConnell, H. *J. Am. Chem. Soc.* **1952**, *74*, 6175−6180.

(31) Tsukruk, V. V.; Reneker, D. H.; Bengs, H.; Ringsdorf, H. *Langmuir* **1993**, *9*, 2141−2144. Tsukruk, V. V.; Bengs, H.; Ringsdorf, H. *Langmuir* **1996**, *12*, 754−757.

(32) Markovitsi, D.; Bengs, H.; Ringsdorf, H. *J. Chem. Soc., Faraday Trans.* **1992**, *88*, 1275−1276.

(33) Mendicuti, F.; Saiz, E.; Bravo, J.; Mattice, W. *Polym. Int.* **1995**, *36*, 137−146.

(34) Markovitsi, D.; Pfeffer, N.; Charra, F.; Nunzi, J.-M.; Bengs, H.; Ringsdorf, H. *J. Chem. Soc., Faraday Trans.* **1993**, *89*, 37−42.

(35) Boden, N.; Bushby, T. J.; Clements, J.; Luo, R. *J. Mater. Chem.* **1995**, *5*, 1741−1748.

(36) (a) Mendicuti, F.; Martín, O.; Bello, P.; Heaton, N. J. Unpublished results. (b) Bello, P.; del Campo, A.; Riande, E.; Herradón, B.; Heaton, N. J. Manuscript in preparation.

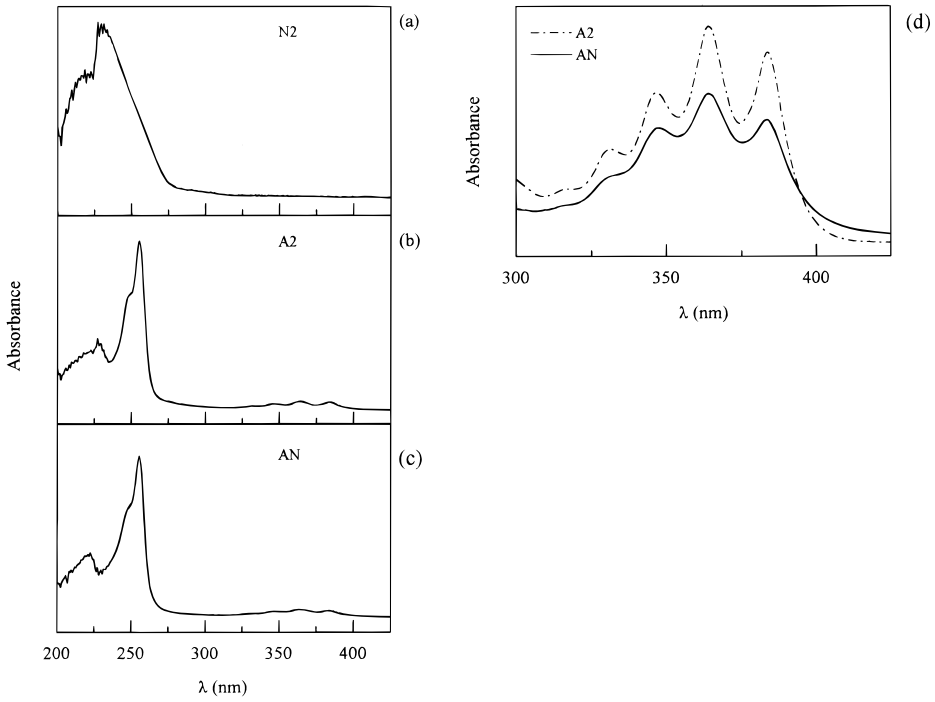

Figure 10. UV region of absorption spectra of (a) **N2**, (b) **A2**, and (c) **AN** in dichloromethane solution (10^{-5} mol dm^{-3}). No bands are observed in the visible region (see text). The 360-nm bands due to the anthracene groups in **A2** and **AN** are compared in part d.

2-methylpropane.[36b] This compound gives a colorless solution in a variety of solvents, including benzene, and also exhibits no charge-transfer absorption band.[36b] A more detailed investigation of the fluorescence behavior of these materials will hopefully shed more light on the nature and dynamics of this type of intramolecular complexation. Further evidence which contradicts the hypothesis that charge-transfer interactions are responsible for the complex formation is provided by the solvent dependence of the conformational energies. It was demonstrated above that the occupation of gauche states of the central C−C bonds in **AN** decreases on changing the solvent from apolar benzene to the highly polar DMSO. This implies that the U-shaped conformers, which give rise to the intramolecular complexes, are destabilised by increasing the dielectric constant of the solvent. Charge-transfer complexes, by their very nature, possess high dipole moments and are stabilized by polar solvents. Analysis of the vicinal coupling constant data for **AN** indicates just the opposite effect. While these results cannot be regarded as conclusive proof for the total absence of charge-transfer interactions in **AN**, the weight of evidence clearly suggests that such interactions, if they occur at all, are not primarily responsible for formation of the intramolecular complex.

It has been shown that the quadrupole interaction can play an important role in determining the overall potential betwen planar aromatic molecules.[6,8] As far as we are aware, the role of intramolecular quadrupole interactions has not been investigated in any depth, although it has been suggested that they could play an important role in stabilizing intercalated smectic phases.[5] Quadrupole interactions between large planar aromatic groups undoubtedly exist and may be sufficiently large to contibute significantly to the intramolecular potentials in the aromatic diesters of 2-methyl-1,3-propanediol studied here. The quadrupole interaction between two cylindrically symmetric molecules has been discussed by several authors.[6,37] The assumption of cylindrical symmetry for the quadrupole tensors of the dinitrobenzoyl and anthracenecarbonyl groups should be regarded as a simplifying approximation. However, in view of the limited information content of the experiments and the absence of literature values for the quadrupole tensor components for these groups, the approximation is justified. We note that similar assumptions have been applied to describe the quadrupole interactions of substituted phenyl groups.[38] For the particular case of a pair of disc-like molecules in the parallel orientation (i.e., with normals to the disc planes parallel), the quadrupole interaction may be expressed as

$$U_Q = \frac{3Q_1Q_2}{2\pi\epsilon r^5}P_4(\cos\theta) \qquad (10)$$

where Q_1 and Q_2 are the quadrupole moments of molecules 1 and 2, r is the distance between them, θ is the angle between the disc plane normal and the vector connecting the centers of the two molecules and ϵ is the dielectric constant of the medium. Evidently, the sign of the interaction is determined by the product of the two quadrupole moments, Q_1Q_2, while the orientation dependence is given by the fourth-rank Legendre polynomial, $P_4(\cos\theta) = (35\cos^4\theta - 30\cos^2\theta + 3)/8$. The magnitude of the interaction is a maximum for $q = 0$, that is when the intermolecular vector is normal to the disc planes. Therefore, for two similar molecules, this face-to-face arrangement has a high energy and a low probability. In contrast, for two unlike molecules with quadrupole moments of opposite sign, this arrangement has the lowest energy.[6] Analysis of the NOE data for **AN**, presented in section C, yielded a structure for the intramolecular complex in which the dinitrophenyl group is centered directly above the central ring of the anthracenyl group, with the two aromatic planes almost parallel. Allowing for some distortion due to constraints imposed by the connecting chain, this is entirely consistent with the lowest energy structure

(37) Vega, C.; Gubbins, K. E. *Mol. Phys.* **1992**, *72*, 881−895. Stone, A. J. In *The Molecular Physics of Liquid Crystals*; Luckhurst G. R., Gray, G. W., Eds.; Academic Press: London, 1979; Chapter 2.

(38) Luhmer, M.; Bartik, K.; Dejaegere, A.; Bovy, P.; Reisse, J. *Bull. Soc. Chim. Fr.* **1994**, *131*, 603−606.

expected if an attractive quadrupole interaction dominates the potential between the two unlike aromatic groups. The observed solvent dependence of the gauche energies of the central C−C bonds is in qualitative—although not quantitative—agreement with eq 10, which predicts a $1/\epsilon$ dependence for the quadrupole interaction. For the intramolecular complex in **AN**, solvent molecules must be expelled from the region between the aromatic planes and the effective ϵ is presumably closer to ϵ_0, the free space value. We note that for two groups or molecules in very close proximity, higher order multipole terms may become important in the overall interaction energy, particularly when electron exchange takes place.[39] Neglect of these terms is strictly only valid for well-separated molecules or groups. Whether this condition is entirely satisfied for the intramolecular complex in **AN** is not clear. However, for present purposes, eq 10 provides a useful first-order description of the interaction which accounts for the observed results.

It is interesting at this point to compare our results with other estimates for quadrupolar interaction energies. Unfortunately, quantitative experimental studies of quadrupole interactions are very scarce. The majority of experimental work to date has focused on the benzene/hexafluorobenzene mixture, which represents the simplest system for which quadrupolar interactions are known to play a fundamental role. To make any comparisons between our work and these previous studies, we first require estimates for the quadrupole moments, Q, for the anthracenecarbonyl and 3,5-dinitrobenzoyl groups. For present purposes, suitable estimates are provided by considering the model compounds, anthracene and 1,3,5-trinitrobenzene. Semiempirical MO calculations, combined with experimental data yield a value of $Q = -61 \times 10^{-40}$ C m^2, about twice the magnitude (-29×10^{-40} C m^2) of that for benzene.[40] We are not aware of any estimates of Q for 1,3,5-trinitrobenzene or other nitro-substituted benzenes suitable as model compounds for the dinitrobenzoyl group. A simple calculation based on the notion of partial atomic charges has been performed for trinitrobenzene (TNB), which yields the sign of the quadrupole moment and a crude estimate of its magnitude relative to that of benzene (B). An absolute value for the quadrupole moment is then given by $Q(\mathrm{TNB}) = [S(\mathrm{TNB})/S(\mathrm{B})] \times Q(\mathrm{B})$, where $Q(\mathrm{B})$ is the experimental quadrupole moment of benzene and $S(\mathrm{TNB}) = \sum e_i r_i^2$. The sum is carried out over all atoms, i, in 1,3,5-trinitrobenzene, with partial charge e_i and distance r_i from the center of the ring. An analogous calculation is performed for benzene to obtain $S(\mathrm{B})$. Since we employ standard planar geometry for the aromatic groups, this approach ignores the three-dimensional nature of the charge distribution. The results must therefore be regarded as first-order approximations. It might be expected, however, that some of the errors introduced by the assumption of planarity are canceled by taking the ratio $S(\mathrm{TNB})/S(\mathrm{B})$. We note that a similar approach has been employed to obtain absolute values for quadrupole moments from theoretical MO calculations. [40] Using values of $e(\mathrm{C}) = +0.18$, $e(\mathrm{N}) = +0.16$, and $e(\mathrm{O}) = -0.17$ for CNO_2 groups and $e(\mathrm{C}) = -0.1$ and $e(\mathrm{H}) = +0.1$ for aromatic CH bonds, together with standard values for bond lengths and angles, we obtain $[S(\mathrm{TNB})/S(\mathrm{B})] = -3.5$ and hence $Q(\mathrm{TNB}) = +105 \times 10^{-40}$ C m^2. As expected, we find that the quadrupole moments of 1,3,5-trinitrobenzene and, by inference, the 3,5-dinitrobenzoyl group are of opposite sign to that of anthracene and the anthracenecarbonyl group. According to the partial charge approach, the quadrupole moments for the dinitrobenzoyl and anthracenecarbonyl groups are expected to be slightly smaller than these estimates derived for the model compounds, yet somewhat larger than those for benzene and hexafluorobenzene. If the quadrupole interaction governs the benzene/hexafluorobenzene complex formation, it can also be expected to influence the intramolecular potential in **AN**.

A study of magnetic field induced dipolar coupling constants[41] indicates a free energy of formation of 6 kJ mol^{-1} for the benzene/hexafluorobenzene dimer. This quantity is determined primarily by the intermolecular quadrupole interaction, which favors the face-to-face planar arrangement for the dimer. It may be compared with the value of 4.0 ± 1.5 kJ mol^{-1} for the intramolecular complex formation in **AN** determined from the vicinal coupling constants in this study. Although the systems compared are obviously rather different, the energies involved in complex formation should be of a similar magnitude if they both derive primarily from the quadrupolar interaction. The fact that the two results coincide reasonably well provides further support for the hypothesis that quadrupolar interactions govern the intramolecular complex in **AN**. The slightly smaller values obtained for **AN** may reflect the constraints imposed on the complex structure by the spacer chain which does not permit the two aromatic groups to minimize the quadrupolar interaction energy.

An estimate of the pure quadrupole interaction energy can also be obtained from eq 10. Using the estimates for the quadrupole coupling constants discussed above, we obtain values for U_Q ($\theta = 0$) about an order of magnitude greater than the energy differences observed experimentally in this study. Of course, the experimentally observed energies represent "compromise structures" determined by all the various contributions to the overall intramolecular potential. Minimization of the quadrupolar interaction energy is only achieved at the expense of other terms, in particular those which govern the flexible chain configuration and the short-range repulsive interactions. Taking account of these effects, it is certainly reasonable to rationalize the observed conformational energy differences in AN with the quadrupole interaction, as described in eq 10. Quantum chemical analysis, together with more exhaustive spectroscopic studies, could provide further insight into the nature of the underlying interactions.

Summary

We have shown that the unsymmetrical diester, **AN**, forms a stable intramolecular complex in which the dinitrophenyl and anthracenyl groups face each other in a parallel arrangement, a distance of about 0.3 nm apart. The spacer chain joining the two aromatic groups adopts a U-shaped conformations in which the two central C−C bonds are in gauche states. The energies of these states have been determined by analysis of the vicinal coupling constants in benzene and DMSO solvents. In benzene, we estimate values of about −4000 J mol^{-1}, while in DMSO, values of about −3000 J mol^{-1}, relative to the trans state, are obtained. Since these gauche conformations may be associated predominantly with the U-shaped conformations, their energies provide an estimate of the stabilization energy of the complexation. On the basis of the evidence from NMR and UV−vis spectroscopy, we suggest that the intramolecular complex is due to an attractive quadrupolar interaction between the unlike

(39) Scholes, G. D.; Ghiggino, K. P. *J. Phys. Chem.* **1994**, *98*, 4580−4590, Markovitsi, D.; Germain, A..; Millié, P.; Lécuyer, P.; Gallos, L. K.; Argyrakis, P.; Bengs, H.; Ringsdorf, H. *J. Phys. Chem.* **1995**, *99*, 1005−1017.

(40) Chablo, A.; Cruickshank, D. W. J.; Hinchcliffe, A.; Munn, R. A.. *Chem. Phys. Lett.* **1981**, *78*, 424−427. (b) Battaglia, M. R.; Buckingham, A. D.; Williams, J. H. *Chem. Phys. Lett.* **1981**, *78*, 421−423.

(41) Laatikainen, R.; Santa, H.; Hiltunen, Y.; Lounila, J. *J. Magn. Reson. A* **1993**, *104*, 238−241.

aromatic groups. The possibility that van der Waals interactions provide the stabilization of the complex can be ruled out since the symmetric diesters, **N2** and **A2**, display no similar behavior. Similarly, we find no evidence for the existence of a charge-transfer complex in **AN**. In fact, the observed relative destabilization of the U-shaped conformers in the polar solvent, DMSO, is entirely inconsistent with the hypothesis that the intramolecular complex results from charge-transfer interactions. Taking account of all the evidence provided by NMR and UV−vis spectroscopy, we propose that quadrupole interactions are responsible for the formation of the intramolecular complex. If the quadrupole moments of the dinitrobenzoyl and anthracenecarbonyl groups are of opposite sign, the interaction favors structures in which the two aromatic planes are parallel and directly facing each other.[6] Analysis of NOE data for **AN** yields a structure for the complex which is consistent with this arrangement. In contrast, for symmetric dimers, the quadrupole interaction is repulsive in these configurations, opposing the attractive van der Waals interactions. Presumably it is for this reason that no intramolecular complex is observed for **N2** or **A2**.

In view of these results, it is interesting to speculate on the role of quadrupole interactions in other similar intramolecular or intermolecular complexes formed between aromatic groups. In particular, the interpretation of induced mesophases in terms of charge-transfer interactions[3,4] is questioned.[6] While the existence of charge-transfer complexes in these systems is beyond doubt, it is not clear whether it is these interactions which are primarily responsible for the stabilization of the mesophases. In this study we have demonstrated that intramolecular complexes can be formed between unlike planar aromatic groups apparently without the assistance of charge transfer. If, as we suggest here, quadrupole interactions are large enough to give rise to stable intramolecular complexes, it is natural to question whether they might not also provide the stabilization energy for induced mesophases in doped discotic systems.

The interaction between the anthracenecarbonyl and dinitrobenzoyl groups in **AN** dominates the intramolecular potential and determines the conformational distribution of the connecting spacer chain. Incorporating these or similar groups into suitable polymer structures is straightforward and could lead to a range of hitherto unexplored materials with controlled conformation and intramolecular discotic-like structures. Work along these lines is currently underway in our laboratory.

Acknowledgment. This paper is in memory of Juan Salort. We thank F. Mendicuti, O. Martín, and E. Saiz (University of Alcalá, Spain) and E. Riande (ICYTP, Madrid, Spain) for helpful discussions concerning fluorescence, dipole moments, and conformational behaviors in aromatic diesters. We are particularly grateful to G. R. Luckhurst (University of Southampton, U.K.) for invaluable comments regarding quadrupole interactions and for kindly providing us with a preprint of ref 6. This work was funded in part by Grant PB95-0134-C02-01 of the Spanish Ministerio de Educación y Cultura. A. del Campo thanks the Fundación Ramón Areces for financial support.

Supporting Information Available: ^{1}H NMR, ^{13}C NMR, and mass spectra of **N2**, **N1**, **A2**, **AN**, and **M2** (41 pages, print/PDF). See any current masthead page for ordering information and Web access instructions.

JA980528S